Spatiotemporal decoupling of littoral and lacustrine geosmin dynamics: Implications for early warning in drinking water reservoirs

Yuying Gui[a,b,#] Tengxin Cao[b,f,#] Jie Yang[c] Jihui Qin[d] Ming Su[b,f,*] Ziyi Yang[b,f]

Qi Zhang[e] Yufan Ai[b,f] Jiao Fang[b] Yingjie Li[b,f] Yuanhong Xiao[d] Zhixiang Hao[c]

Zhengyan Li[a] Min Yang[b,f]

[#] These authors contributed equally to this work.

[a] College of Environmental Science and Engineering, Ocean University of China, Qingdao 266100, China.

[b] Key Laboratory of Environmental Aquatic Chemistry, State Key Laboratory of Regional Environment and Sustainability, Research Center for Eco-Environmental Sciences, Chinese Academy of Sciences, Beijing 100085, China.

[c] Tianjin Hydraulic Research Institute, Tianjin 300061, China.

[d] Tianjin Yuqiao Reservoir Authority, Tianjin 301900, China.

[e] Institute of Hydrobiology, Chinese Academy of Sciences, Wuhan 430070, China.

[f] University of Chinese Academy of Sciences, Beijing 100049, China.

[*] Corresponding to: Ming Su (mingsu@rcees.ac.cn)

Abstract

The relationship between cyanobacterial niche characteristics and the transport dynamics of harmful metabolites to drinking water intakes remains poorly understood. This study integrated a national survey with a five-year high-frequency monitoring program to characterize these dynamics, focusing on the potent odorant geosmin. The national investigation revealed that 14% of surveyed sites exceeded the odor threshold of 10 ng L^{-1}, indicating a non-negligible risk. In the YQ Reservoir, *Planktothrix agardhii* was identified as a primary producer. Monitoring revealed a distinct spatiotemporal decoupling: shallow littoral zones functioned as production centers where *P. agardhii* biomass peaked 8 days prior to the lacustrine intake. Time-lagged correlation analysis indicated that littoral biomass predicts intake geosmin concentrations with a 5-week lead time (R^2 = 0.41). Ammonium was identified as the key regulatory factor, exhibiting its strongest correlation with geosmin in littoral zones (R^2 = 0.37), though this linkage attenuated during transport. This proposed mechanistic transport model and tiered framework shift surveillance from reactive intake sampling to proactive littoral sentinel stations, establishing a critical predictive window for preventive intervention in reservoir-dependent water supplies.

Keywords: *Geosmin*, *taste and odor*, *Early warning*, *Planktothrix agardhii*, *Spatiotemporal decoupling*

1 Introduction

The increasing frequency and intensity of harmful cyanobacterial blooms (CyanoHABs) in surface waters, driven by climate change and intensified anthropogenic activities, represent a significant global threat to water security (Feng et al., 2021; Heisler et al., 2008; Huisman et al., 2018; O'neil et al., 2012; Paerl et al., 2001; Paerl and Paul, 2012; Woolway et al., 2020). While CyanoHABs in eutrophic shallow lakes have been extensively characterized (Kosten et al., 2011; Paerl et al., 2011; Reinl et al., 2022; Rousso et al., 2020; Xu et al., 2009; Zhang et al., 2023), research in reservoir systems remains comparatively limited. In these critical drinking water resources, CyanoHABs directly jeopardize water safety through the production of toxins (Carmichael et al., 2001; Merel et al., 2013; Plaas and Paerl, 2020) and taste-and-odor (T&O) compounds (Burlingame et al., 2017; Lin et al., 2018; Su et al., 2015; Yang et al., 2008). Approximately half of China's source-water reservoirs experience recurrent algal-derived T&O episodes (Sun et al., 2014). Unlike chemical contaminants, cyanobacterial populations exhibit exponential growth under favorable conditions (Asato, 2003; Mehnert et al., 2010), resulting in rapid metabolite release (Ai et al., 2025; Singh et al., 2005) that often exceeds the treatment capacity of conventional water utilities (Cerón-Vivas et al., 2022; Mustapha et al., 2021; Srinivasan and Sorial, 2011).

Managing CyanoHABs in reservoirs involves distinct challenges due to spatial and hydraulic complexity, which results in less predictable ecological regimes than those in natural lakes (Dordoni et al., 2023; Thornton, 1984). Conventional monitoring strategies, typically concentrated at lacustrine intakes near dams, often fail to capture the heterogeneous distribution of algal biomass and metabolites. Furthermore, the limited hydraulic residence time between the intake and the treatment plant provides an insufficient operational window for intervention. Littoral zones, with their shallow depth, generally warm earlier in spring and maintain higher light availability throughout the water column compared to deeper offshore areas (Bracchini et al., 2009). These nearshore regions also exhibit stronger sediment–water coupling, evident in diffusive nu-

trient fluxes and episodic wind-driven resuspension, which significantly enhance internal nutrient supply (Akbarzadeh et al., 2025; Qin et al., 2006). Together, these physicochemical factors (Cefalì et al., 2016; Zohary and Gasith, 2014) create an optimal ecological niche that supports the early proliferation of cyanobacteria. Despite their potential as sentinel sites, these areas are frequently under-monitored, and the mechanistic linkages between littoral zone dynamics and downstream water quality at intakes remain insufficiently quantified.

Geosmin and 2-methylisoborneol (MIB) are the primary terpenoid T&O compounds synthesized by cyanobacteria (Jüttner and Watson, 2007; Watson, 2003). Their low molecular weight and chemical stability allow them to penetrate conventional treatment barriers and persist in distribution networks (Lin et al., 2018; Zamyadi et al., 2015). While MIB episodes in China have been well studied and managed through hydraulic controls (Lu et al., 2023; Su et al., 2015), geosmin episodes are increasing in frequency across Northern Hemisphere reservoirs (Qiu et al., 2023; Wu et al., 2022). The high phylogenetic diversity of geosmin-producing taxa (AWWA, 2010) complicates the identification of biological sources and the development of targeted management strategies, emphasizing the need for research into the ecological niches and growth dynamics of these organisms in littoral zones.

This study analyzes recent national survey data to characterize the occurrence of geosmin across China's drinking water sources and presents a five-year, spatially resolved investigation of a representative reservoir. By integrating water chemistry, molecular profiling, and statistical modeling, this research examines the spatiotemporal decoupling between cyanobacterial communities in littoral zones and concentrations at the lacustrine intake. The objectives are to identify the primary cyanobacterial taxa responsible for geosmin production and to demonstrate how population dynamics within littoral hotspots determine downstream odor levels. This work provides an evidence-based framework for shifting from reactive treatment toward proactive, risk-based management of cyanobacterial T&O threats.

2 Materials and methods

2.1 Study area and sampling design

National-scale geosmin survey. This study compiles geosmin concentration data from drinking water sources across China, representing an extensive national assessment of this odorant. The dataset integrates long-term monitoring results with high-quality measurements from established literature, including a survey of 33 reservoirs in Guangdong province (Zhou et al., 2024). To improve data comparability, only quantitative geosmin data from raw water samples analyzed using GC–MS-based methods were included. For risk assessment, a uniform exceedance threshold of 10 ng L^{-1} was applied across all sites, and values reported below method detection limits (MDLs) were treated as non-exceedance records in the exceedance-rate analysis. In total, geosmin data from 214 distinct sampling sites were analyzed to characterize spatial heterogeneity and nationwide occurrence patterns.

Intensive monitoring at a reservoir in northern China. YQ Reservoir is a large, river-type reservoir located in northern China, with a total storage capacity of approximately 1.559 billion m^3, and serves as an important drinking water source for a major metropolitan area in northern China (Xu et al., 2014; Zhai et al., 2017). In recent years, the reservoir has experienced recurrent seasonal taste-and-odor episodes (Cai et al., 2017; Qiu et al., 2021). Based on bathymetric and hydrodynamic gradients, seven sampling sites (YQ01–YQ07) were established along a littoral-to-lacustrine transect. Site YQ01, located in the deep lacustrine zone (maximum depth of approximately 12 m), was monitored using integrated water column sampling. Sites YQ02–YQ07 were situated in shallower littoral and transitional zones (water depth 2–4 m), where surface water samples were collected because the shallow depth and frequent mixing were unlikely to produce persistent vertical stratification (Holgerson et al., 2022). High-frequency sampling (2–3 times per week) was conducted during the annual odor season from 2019 to 2024. Samples for geosmin analysis, water chemistry, and phytoplankton assessment were collected concur-

rently, stored at 4 °C in the dark, and processed within 24 hours.

2.2 Analytical methods

Geosmin analysis. Geosmin concentrations were determined via headspace solid-phase microextraction (HS-SPME) coupled with gas chromatography–mass spectrometry (GC-MS; Agilent 6890GC-5973MSD) following established protocols (Su et al., 2015). The method detection limit (MDL) for geosmin was 1 ng L^{-1}.

Physicochemical parameters. Water temperature, pH, dissolved oxygen (DO), and turbidity were recorded *in-situ* using a multiparameter sonde (EXO2, Xylem, USA). Concentrations of ammonium (NH_4^+-N), total nitrogen (TN), and total phosphorus (TP) were determined spectrophotometrically following Chinese national standard protocols. Specifically, TN and TP were quantified after alkaline potassium persulfate digestion (HJ 636-2012 and GB/T 11893-1989, respectively). NH_4^+-N was measured using the Nessler's reagent method (HJ 535-2009).

Phytoplankton analysis. At each sampling station, a 1 L water sample was collected and immediately fixed with Lugol's iodine solution (1% final concentration). After 48 h of static sedimentation, the samples were concentrated to a final volume of 50 mL (Hawkins et al., 2005). For phytoplankton identification and enumeration, a 0.1 mL aliquot of the concentrate was transferred to a Sedgewick–Rafter counting chamber. Phytoplankton were identified and counted under an upright microscope (Olympus CX23, Tokyo, Japan) at 400× magnification based on morphological characteristics according to (Hu and Wei, 2006). Multiple microscopic fields were examined for each sample. The phytoplankton cell density (C, cells L^{-1}) was calculated using the following equation:

$$C = \frac{n \times V_{con}}{V_{count} \times V_{sample}} \quad (1)$$

where n is the number of cells counted, V_{con} is the concentrated volume (50 mL), V_{count} is the

volume of the counting chamber (0.1 mL), and V_{sample} is the initial sample volume (1 L).

2.3 Molecular characterization and bioinformatics

Molecular identification of geosmin producers. Biomass for molecular analysis was collected on 1.2-µm polycarbonate filters (Millipore) and stored at –80°C. Genomic DNA was extracted using the FastDNA™ Spin Kit for Soil (MP Biomedicals). The *geoA* gene, which encodes geosmin synthase in cyanobacteria, was amplified using functional primers 173AF/173AR (Giglio et al., 2008; Su et al., 2013). Taxonomic identification was performed via PCR amplification of the 16S rRNA gene V4 region (primers 515F/806R). Gene fusion was carried out to combine the (*geoA*) and 16S rRNA gene amplicons using the primers (173AF/806R). Amplicons were verified via agarose gel electrophoresis and subjected to high-throughput sequencing. Representative sequences were taxonomically assigned via BLAST searches, and a maximum-likelihood phylogenetic tree was constructed to confirm the identity of the dominant producer.

Bioinformatics pipeline. The sequencing was performed on the Illumina MiSeq PE300 platform (Illumina Inc., San Diego, USA) (Ravi et al., 2018). The raw paired-end sequences were first merged using FLASH (v1.2.11) and processed for quality filtering within the QIIME2 pipeline (v2022.2) (Bolyen et al., 2019). The UPARSE algorithm (v7.0.1090) was used to remove singletons and chimeras, and the sequences were clustered into Operational Taxonomic Units (OTUs) at a 97% similarity threshold (Edgar, 2013). For the 16S rRNA gene fragments, representative sequences were taxonomically assigned against the SILVA rRNA reference database (release 138) (Quast et al., 2012).

2.4 Data processing and statistical analysis

Temporal aggregation and lagged correlation. Data were aggregated to weekly means to align time series and reduce noise. To investigate time-lagged relationships, weekly geosmin concentrations were shifted forward by i weeks (i = 0–7) and paired with concurrent *Planktothrix*

agardhii biomass. A log–log linear model was applied:

$$\log_{10}(G) = \alpha + \beta \log_{10}(P) + \varepsilon \quad (2)$$

where G is the geosmin concentration (ng L^{-1}) and P is $P.agardhii$ cell density (cells L^{-1}). To minimize low-value interference, only paired observations with geosmin > 2 ng L^{-1} and positive biomass were included. Analysis was restricted to sites with ≥20 valid weekly observations. The coefficient of determination (R^2) was used to identify the optimal lag period (i.e., the early-warning window reported in the main text), and slope significance was evaluated via t-test.

Multivariate and spatial analysis. Principal component analysis (PCA) was performed on standardized variables to explore multivariate relationships. Zone-specific regressions (littoral, transitional, lacustrine) compared the strength of the ammonium–geosmin linkage. Bathymetric data were spatially interpolated via ordinary kriging to illustrate the reservoir's depth gradient. All analyses were conducted in R (version 4.4.2) using the *dplyr*, *lubridate*, *stats*, and *ggplot2* packages.

3 Results

3.1 National survey of geosmin occurrence in drinking water sources

We conducted a nationwide survey of 214 sites across 26 provinces to assess geosmin levels in China's major drinking water sources, including reservoirs and key surface water bodies. Risk potential at each site was evaluated using peak recorded concentrations (Fig. S1). Values varied by more than four orders of magnitude, ranging from non-detectable levels to a maximum of 150 ng L^{-1} in East Coastal China. Across the study area, 14% of sites exceeded the 10 ng L^{-1} odor threshold (Fig. S2). The geospatial distribution showed marked spatial variability; ele-

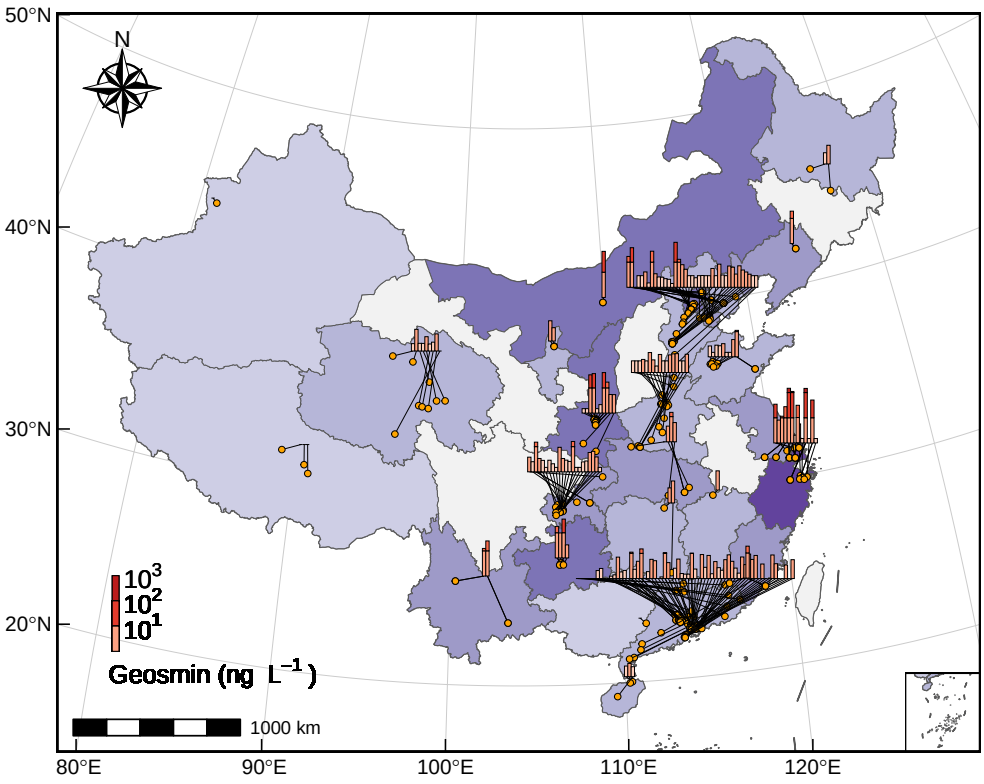

Fig. 1: A multi-scale visualization of geosmin occurrence: linking individual sampling sites to provincial-level aggregates (Provincial/regional aggregate bars (log-scale binned) connected to individual sampling sites. Beijing-Tianjin-Hebei and Jiangsu-Shanghai-Zhejiang are treated as single units to avoid spatial overlap).

vated geosmin levels were primarily concentrated in eastern and southern China—specifically the Yangtze and Pearl River Deltas and parts of North China. In contrast, concentrations remained low or below detection limits throughout the northwest (e.g., Tibet, Xinjiang, and Qinghai) and certain central provinces, indicating a clear longitudinal gradient. These results identify geosmin as a pervasive odorant affecting drinking water quality across diverse climatic and geographic zones in China.

3.2 Seasonal and interannual dynamics in YQ Reservoir

High-frequency monitoring was conducted at the primary intake (site YQ01) of YQ Reservoir from 2019 to 2024 to characterize temporal geosmin variability (Fig. S3). The longitudinal record demonstrates a recurrent seasonal pattern (Fig. 2A, Fig. S4A). Concentrations typically remained

below 5 ng L^{-1} during the spring (April–May), followed by an abrupt increase in June. Primary peaks occurred during the July–August period, with secondary elevations persisting through autumn and early winter (October–December) before a gradual decline. The 10 ng L^{-1} odor threshold was frequently exceeded during the study period. Monthly median values surpassed this threshold in 40% of summer months (July–September) and 100% of autumn/early winter months (October–December), indicating a recurrent odor risk during the warmer half of the year.

Interannual analysis (Fig. 2B) revealed a reduction in geosmin levels following the 2019–2020 monitoring period, which recorded a median concentration of 2.5 ng L^{-1}. Between 2020 and 2024, annual medians stabilized within a range of 5.2 to 10 ng L^{-1}. Statistical differences between years were confirmed by a Kruskal-Wallis test ($\chi^2(4) = 64.3$, $p < 0.001$). These data suggest a shift in baseline conditions or source inputs after the initial year, although seasonal periodicity remained a consistent feature.

3.3 Phytoplankton community dynamics and key cyanobacterial genera

Phytoplankton composition data from YQ Reservoir (site YQ01, 2019–2024) were analyzed to assess the relationship between community dynamics and geosmin occurrence (Fig. 2B). Total phytoplankton biomass (log_{10}-transformed cell density) demonstrated seasonal variability, with minimum values in winter (January–March, ~10^7 cells L^{-1}) followed by an increase starting in April. Biomass peaked during summer (July–September, >10^8 cells L^{-1}) and remained elevated through autumn (October–December) before declining in late winter, a trajectory consistent with observed geosmin fluctuations.

Cyanobacteria dominated the assemblage throughout most of the monitoring period, with peak biomass recorded from June to October. Within this group, filamentous genera associated with geosmin production followed distinct successional patterns. *Planktothrix agardhii* and

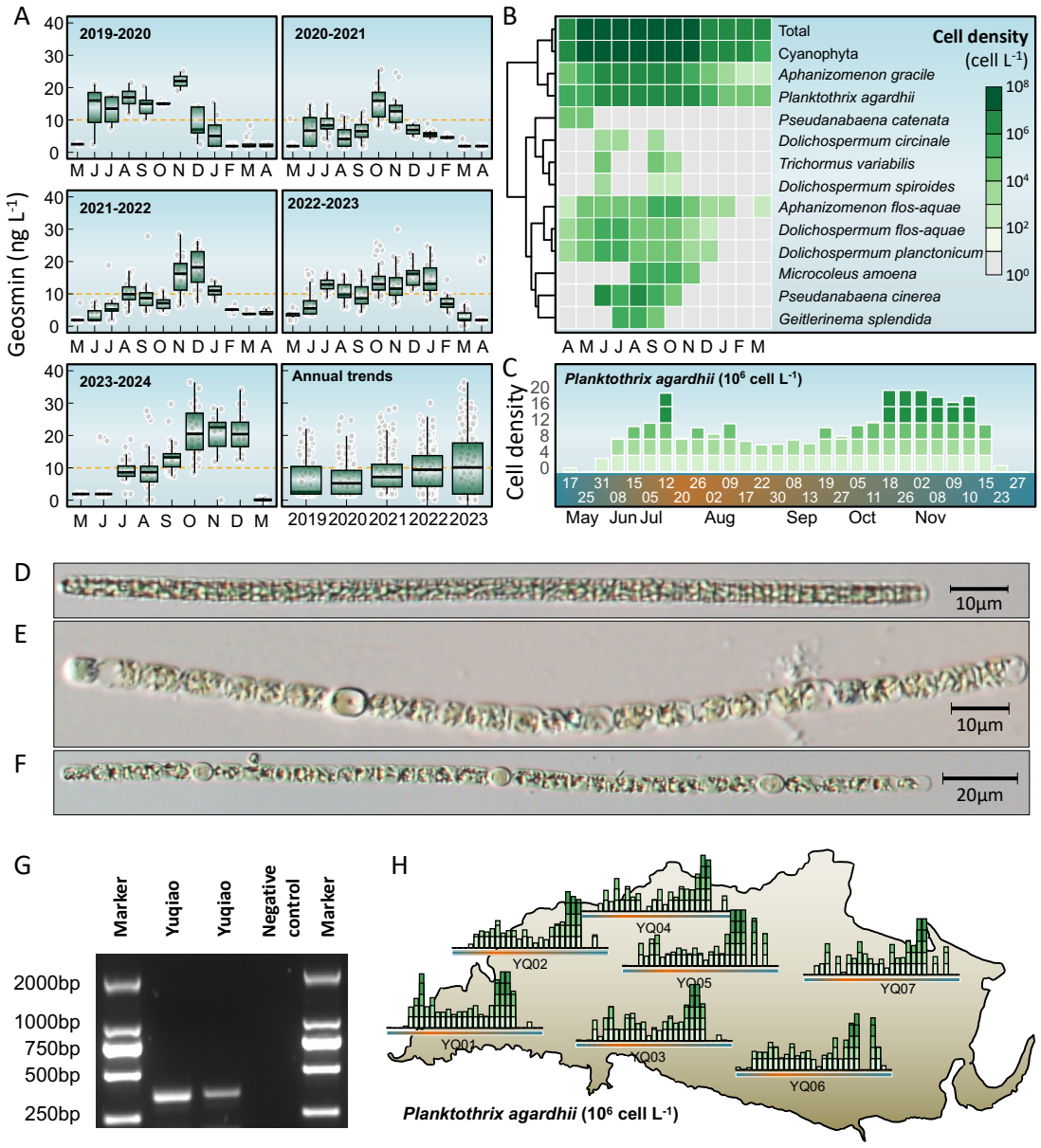

Fig. 2: Long-term dynamics of geosmin and phytoplankton community in YQ Reservoir (2019–2024). (A) Seasonal and interannual variations in geosmin concentrations at the main water intake (site YQ01). (B) Heatmap showing monthly $\log_{10}$-transformed biomass ($\log_{10}(X + 1)$) of total phytoplankton, total cyanobacteria, and key geosmin-producing cyanobacterial genera. (C) Temporal patterns of *Planktothrix agardhii* biomass across sampling sites. (D–F) Microscopic images of primary geosmin producers (*P. agardhii*, *Dolichospermum* and *Aphanizomenon*). (G) Agarose gel electrophoresis image for the molecular identification of geosmin producers. (H) Spatial mapping of seasonal *P. agardhii* biomass variations at representative sampling sites overlaid on the reservoir map.

Aphanizomenon gracile were present year-round but reached maxima in summer and autumn. In contrast, *Pseudanabaena catenata* was primarily restricted to spring (April–May). Several

Dolichospermum species (e.g., *D. circinale*, *D. flos-aquae*, *D. planctonicum*) and *Aphanizomenon flos-aquae* emerged in late spring, proliferated during summer, and declined by late autumn. Other taxa, including *Trichormus variabilis*, *Microcoleus amoenus*, and *Pseudanabaena limnetica*, occurred sporadically, with peaks confined to specific intervals between June and August.

The synchronization of elevated geosmin concentrations with high cyanobacterial biomass—particularly during blooms of *Planktothrix*, *Dolichospermum* and *Aphanizomenon*—points to a biological origin for the odor episodes. The temporal succession of these specific taxa likely drives the characteristic bimodal geosmin peaks observed during the summer and autumn months.

3.4 Identification and spatiotemporal distribution of the primary geosmin producer

Screening of 16S rRNA and *geoA* gene sequences identified the genera *Planktothrix*, *Dolichospermum*, and *Aphanizomenon* as the primary geosmin producers in YQ Reservoir (Fig. 2D-2G). Due to the high diversity and dynamic succession of filamentous cyanobacteria observed over the five-year monitoring period, taxonomic identification at the species level remains inconclusive based on current evidence. For subsequent analysis, *P. agardhii* was selected as the representative taxon for subsequent analysis because it showed a more persistent temporal pattern than other candidate producers across the monitoring period (Fig. 2B–C) and exhibited the strongest correlation with geosmin concentrations (Fig. S4B).

Spatial monitoring in 2023 demonstrated a clear biomass gradient; littoral sites (YQ03, YQ04, YQ06, and YQ07, Fig. S3) maintained significantly higher cell densities than the lacustrine site (YQ01). Maximum biomass reached 5.6×10^7 cells L^{-1} at littoral locations, nearly double the peak of 3.9×10^7 cells L^{-1} recorded at the lacustrine abstraction point. Biomass exceeded the 2×10^7 cells L^{-1} threshold in 8.7% of littoral samples, compared to 8.6% at YQ01. Unlike the ephemeral peaks of other cyanobacteria, *P. agardhii* persisted throughout the warm season (Fig. 2C).

The progression of bloom events (≥2 × 10^7 cells L^{-1}) followed a spatial sequence from the littoral zone toward the dam (Fig. 2H). For example, YQ05 reached this threshold 8 days before YQ01. This temporal lag suggests that littoral zones function as primary proliferation centers, with subsequent advection driving the geosmin peaks observed at the lacustrine intake.

3.5 Distinct spatiotemporal patterns of two geosmin episodes

Two distinct odor episodes were identified in YQ Reservoir during 2023 (April–August and August–December). Spatial mapping of monthly average geosmin concentrations at seven representative sites revealed contrasting trajectories between littoral and lacustrine regions (Fig. 3).

During the first episode (April–August), littoral sites (YQ02, YQ03, YQ04, YQ06, and YQ07) recorded elevated concentrations in spring (April–June), ranging from 0 to 21.2 ng L^{-1}. These values declined by August to between 0.6 and 5.8 ng L^{-1}. In contrast, the lacustrine site (YQ01) and the transitional site (YQ05) exhibited a delayed response; concentrations increased progressively from April minima to reach a peak in August at 8.5 ng L^{-1}.

The second episode (August–December) showed a reversed spatiotemporal gradient. Littoral sites reached peak concentrations in October, ranging from 0 to 36.4 ng L^{-1}, before decreasing by December. Conversely, the lacustrine site (YQ01) exhibited a monotonic increase throughout the period, reaching 24.2 ng L^{-1} in December. Site YQ05 demonstrated an intermediate transition, with concentrations declining in November.

These divergent trajectories (Fig. 3) indicate a systematic spatiotemporal decoupling: littoral zones demonstrate earlier onset and decline during both episodes, while the lacustrine region shows delayed and prolonged elevations. This pattern reflects the integrated effects of initial production in littoral hotspots and subsequent advective transport toward the central reservoir.

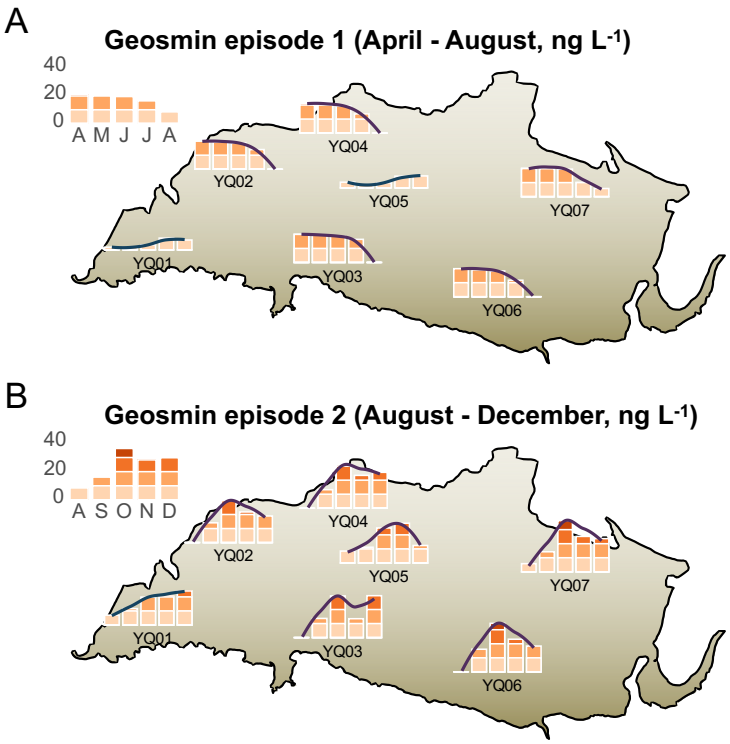

Fig. 3: Spatial mapping of monthly mean geosmin concentrations during Episode 1 (April–August, A) and Episode 2 (August–December, B) in YQ Reservoir.

3.6 Predictive relationship between *Planktothrix agardhii* dynamics and geosmin episodes

Time-lagged correlation analyses were performed between *Planktothrix agardhii* biomass and geosmin concentrations at the near-littoral site YQ05 and the lacustrine site YQ01 (Fig. 4A, Fig. S8). The analysis demonstrated divergent temporal coupling between the two locations. At YQ05, the strongest correlation ($R^2 = 0.5$, $p < 0.001$) occurred at zero lag, indicating that geosmin levels fluctuated synchronously with local *P. agardhii* density. In contrast, the correlation at the lacustrine site YQ01 was weakest at zero lag but increased with time, peaking at a 5-week lag ($R^2 = 0.41$, $p < 0.001$). This offset indicates that *P. agardhii* biomass functions as a concurrent indicator in the littoral production zone but acts as a leading indicator for geosmin risk at the distal lacustrine intake.

Regression models were established using the optimal lag periods for each site (Fig. 4B). For YQ05 (zero lag), the relationship followed the equation: $\log_{10}(\text{geosmin}) = 0.244 + 0.288 \times \log_{10}(\textit{P. agardhii}$ biomass). For YQ01 (5-week lag), the model was: $\log_{10}(\text{geosmin}) = 0.558 + 0.196 \times \log_{10}(\textit{P. agardhii}$ biomass). The higher slope observed at YQ01 suggests a potential amplification of geosmin concentrations during transport from littoral zones to the reservoir center.

Bi-weekly time series further illustrate this temporal phasing (Fig. 4C). At YQ05, *P. agardhii* and geosmin peaks were closely aligned, whereas at YQ01, biomass peaks preceded major odor episodes by approximately 6.7 weeks. This consistent lag serves as a predictive window; when *P. agardhii* biomass at YQ05 exceeded 5.0×10^7 cells L^{-1}, geosmin at the lacustrine intake surpassed the 10 ng L^{-1} threshold within 4–6 weeks in 61.9% of observations. These results support the use of near-littoral monitoring for forecasting odor risks at central abstraction points.

3.7 Environmental drivers of geosmin and proposed transport pathway

Clear spatial gradient in nutrient loading and algal response was observed in YQ Reservoir (Fig. S9). The littoral sites exhibit the highest vulnerability to organic enrichment, particularly during the summer. In this period, the littoral zone reaches a peak mean Chl-a of 0.072 mg L^{-1}, which is significantly higher than the 0.061 mg L^{-1} observed in the lacustrine zone. This spatial disparity is mirrored in the Chemical Oxygen Demand (COD) and turbidity levels, with littoral sites showing higher COD (5.87 mg L^{-1}) and lower Secchi Disk transparency (50.6 cm) than the deeper water sites. In contrast, the lacustrine zone displays higher stability regarding immediate organic surges but acts as a major sink for nitrogen. During winter, the Total Nitrogen (TN) in the lacustrine zone reaches a maximum of 3.56 mg L^{-1}, a level higher than those found in the littoral or transitional areas during the same season. The transitional sites serve as a buffer, with water chemistry parameters like pH and TP typically falling between the littoral peaks and the lacustrine lows.

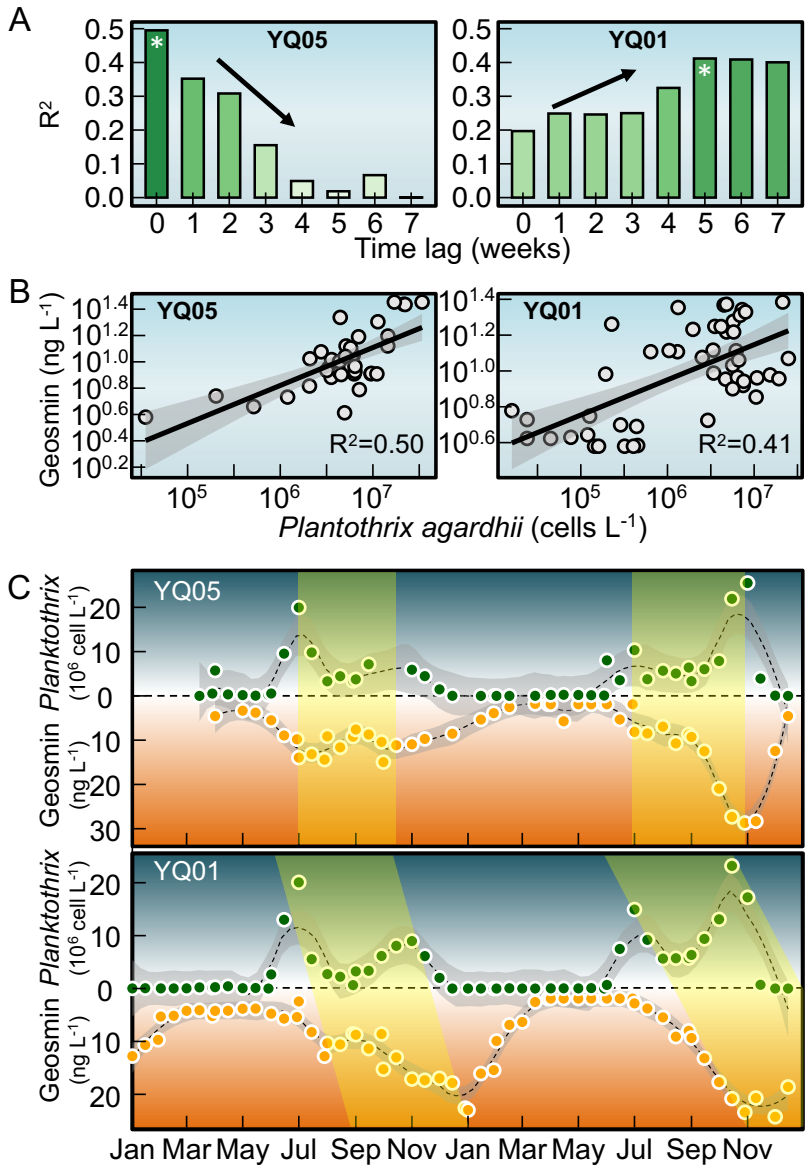

Fig. 4: Time-lagged relationships between *Planktothrix agardhii* biomass and geosmin concentrations at near-littoral and dam sites. (A) Correlation coefficients (R^2) between *P. agardhii* biomass and geosmin at different lag periods (0–5 weeks) for site YQ05 (near-littoral) and YQ01 (dam intake). (B) Linear regression models at optimal lag periods: zero lag for YQ05 and 5-week lag for YQ01. (C) Scatter plots with fitted regression lines showing the quantitative relationships between *P. agardhii* biomass and geosmin at each site.

Principal component analysis (PCA) identified ammonium (NH_4^+-N) as the variable most strongly associated with geosmin variability in the PC1–PC2 plane (Fig. 5A). The first two principal components accounted for 60.6% of total variance. PC1 (43.5%) represented a thermal-nutrient productivity axis, characterized by high loadings for temperature (0.342),

total phosphorus (TP, 0.39), and chlorophyll-a (Chl-a, 0.428). PC2 (17.1%) represented a nitrogen availability axis, dominated by ammonium (-0.449) and total nitrogen (TN, 0.432). Geosmin exhibited moderate positive loadings on both PC1 (0.122) and PC2 (0.229), suggesting that variability is driven by a combination of thermal-nutrient status and nitrogen availability.

Log-log regressions between ammonium and geosmin were performed across three reservoir zones: littoral (YQ02–YQ04, YQ06–YQ07), transitional (YQ05), and lacustrine (YQ01) (Fig. 5B). A clear spatial gradient in correlation strength was observed, with the highest R^2 at littoral sites (0.365), followed by YQ05 (0.203), and the lacustrine site YQ01 (0.035). This attenuation suggests that the ammonium-geosmin linkage is most direct in production zones and undergoes progressive decoupling during transport toward the lacustrine intake.

Based on these results and the observed spatiotemporal dynamics of *Planktothrix agardhii*, a transport pathway for odor episodes is proposed (Fig. 5C). Shallow littoral areas (depths < 4–5 m) serve as primary sites for ammonium accumulation, *P. agardhii* proliferation, and geosmin production. Advective transport then moves cells and dissolved geosmin from these littoral zones through the transitional region (YQ05) to the lacustrine intake (YQ01). This framework integrates the spatial gradient in nutrient-geosmin coupling, the observed temporal lags between zones, and the bathymetric influence on water residence times. These elements provide a mechanistic basis for the origin and delayed manifestation of geosmin episodes at the reservoir's primary abstraction point.

4 Discussion

4.1 Geosmin prevalence in Chinese drinking water sources

National survey data indicate that geosmin contamination is widespread across China's primary drinking water sources, with 14% of sites exceeding the 10 ng L^{-1} odor threshold ((AWWA, 2010)). These results identify geosmin as a pervasive water quality challenge, consistent with obser-

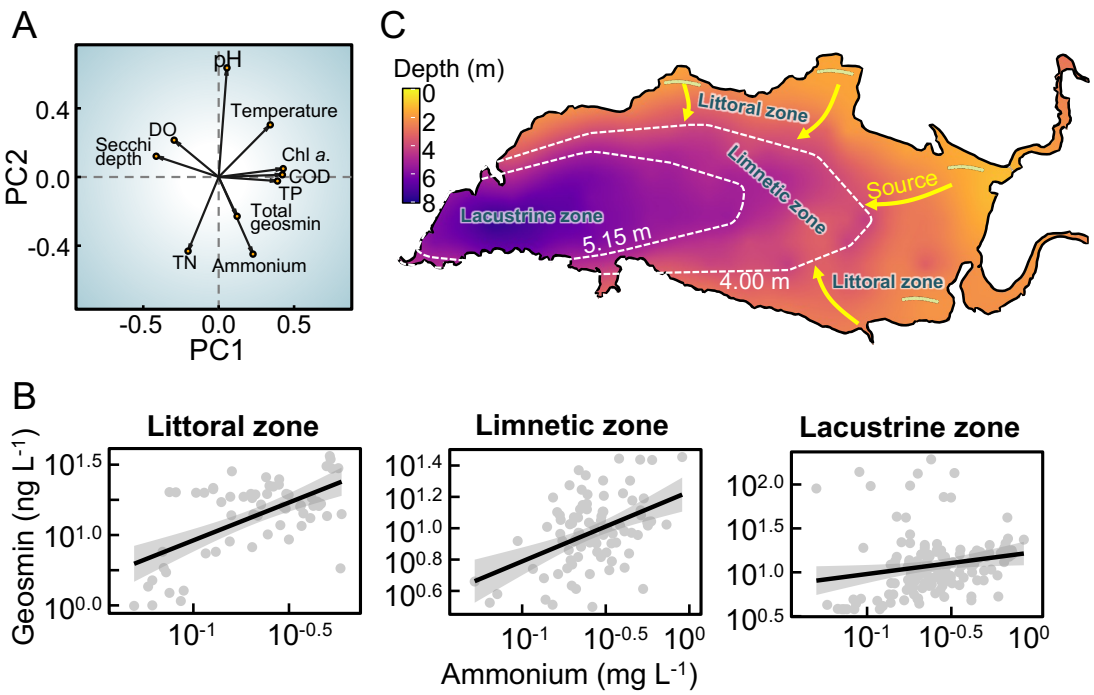

Fig. 5: Environmental drivers and conceptual transport pathway of geosmin in YQ Reservoir. (A) Principal component analysis (PCA) biplot showing relationships between geosmin and key environmental variables. (B) Log-log regressions between ammonium concentration and geosmin across littoral, transitional (YQ05), and dam (YQ01) zones. (C) Bathymetric map of YQ Reservoir depicting the proposed transport pathway from littoral production zones to the central water intake.

vations in other climatological regions (Devi et al., 2021; Lin et al., 2018). The observed spatial heterogeneity—specifically the higher concentrations within the Yangtze and Pearl River Deltas—suggests that regional climatic conditions, watershed land use, and nutrient loading are primary determinants of geosmin risk. Given its low odor threshold and resistance to conventional treatment processes (Cook et al., 2001; Mustapha et al., 2021; Zamyadi et al., 2015), geosmin poses significant operational challenges for water utilities (Srinivasan and Sorial, 2011) and impacts compliance with water safety objectives such as Sustainable Development Goal 6 (Arora and Mishra, 2022). Consequently, these risks drive substantial investment in advanced treatment technologies and proactive source management (Yuan and Hofmann, 2022).

4.2 Littoral zones as production centers and spatiotemporal decoupling

While actinomycetes are established sources of geosmin in freshwater sediments (Gerber, 1979; Gerber and Lechevalier, 1965; Guo et al., 2024; Jensen et al., 1994), the synchronous peaks of *Planktothrix agardhii* biomass and geosmin at littoral sites (R^2 = 0.5), combined with the molecular identification of the *geoA* gene (Fig. 2D, F), confirm a cyanobacterial origin in YQ Reservoir. This supports the consensus that cyanobacteria are the primary biotic source of odorants in well-oxygenated reservoir water columns (Chislock et al., 2021; Hooper et al., 2023; Izaguirre, 1992; Pham et al., 2020; Su et al., 2013; Suurnäkki et al., 2015). Detection of *geoA*-harboring cyanobacteria (Giglio et al., 2011; Giglio et al., 2008; Kutovaya and Watson, 2014) in this oxygenated environment indicates that geosmin is primarily derived from cyanobacterial activity, aligning with studies linking specific blooms to odor episodes globally (Churro et al., 2020; Hayashi et al., 2019; John et al., 2018).

Monitoring data identify littoral zones as critical ecological niches for *P. agardhii* proliferation. The filamentous morphology and low-light adaptation of *P. agardhii* facilitate its dominance in shallow, intermittently mixed littoral environments (Cao et al., 2025; Jia et al., 2019; Komárek and Johansen, 2015; Su et al., 2019). These traits allow for optimal light harvesting under the variable regimes typical of nearshore areas (Scott and Marcarelli, 2012; Zohary and Gasith, 2014). The high correlation between ammonium and geosmin specifically in littoral zones (R^2 = 0.37) points to nitrogen availability from shoreline inputs as a key regulator. The positive correlation observed in situ in the reservoir is consistent with physiological evidence from laboratory studies on geosmin-producing cyanobacteria, which have shown that elevated ammonium concentrations can stimulate cyanobacterial growth and thereby increase overall geosmin production capacity (Canizales et al., 2021; Flores and Herrero, 2005; Saadoun et al., 2001; Yang et al., 2023). Thus, these findings collectively suggest that ammonium availability may serve as an indicator of geosmin production potential. Together, these results support the view that littoral zones act

as the primary production centers for geosmin in YQ Reservoir.

The subsequent weakening of ammonium–geosmin correlation at the lacustrine intake (R^2 = 0.03) reflects the decoupling of biological production from observed concentrations during transport. This spatial decoupling is quantified by the 8-day lag in bloom development between littoral sites and the dam, representing a period of physical advection and continued metabolic accumulation. During this process, the observed delay at the lacustrine intake may partly reflect intracellular geosmin release associated with cell lysis during downstream transport. As *P. agardhii* cells are transported toward the dam, where conditions become less favorable for growth, some cells may undergo lysis and release intracellular geosmin into the water column (Dubourg et al., 2015; Jia et al., 2019). In addition, geosmin concentrations at the lacustrine intake may be further affected by multiple physical and biogeochemical attenuation processes, including dilution through mixing with geosmin-poor water, microbial degradation (Clercin et al., 2021; Hammond et al., 2021; Hoefel et al., 2009), volatilization across the air–water interface (Soyluoglu et al., 2022), and photochemical transformation (e.g., UV degradation) (Kim et al., 2016; Mustapha et al., 2021).

4.3 Implications for monitoring and management

The conceptual mechanism depicted in Fig. 6 illustrates that maximum geosmin production is localized in littoral zones before advective transport through the limnetic zone. This sequence demonstrates a limitation in intake-centric monitoring: by the time geosmin reaches the lacustrine zone, the window for preventive intervention is minimal (Mohanty et al., 2024; Zamyadi et al., 2015). The identified 4–6 week lag between littoral proliferation and lacustrine contamination establishes a quantifiable window for risk mitigation. This estimate is supported by both the 5-week optimal lag identified from weekly lagged-correlation analysis and the 6.7-week delay inferred from the observed time-series pattern, which together indicate a comparable multi-week early-warning interval despite differences in method. By deploying littoral sentinel sites,

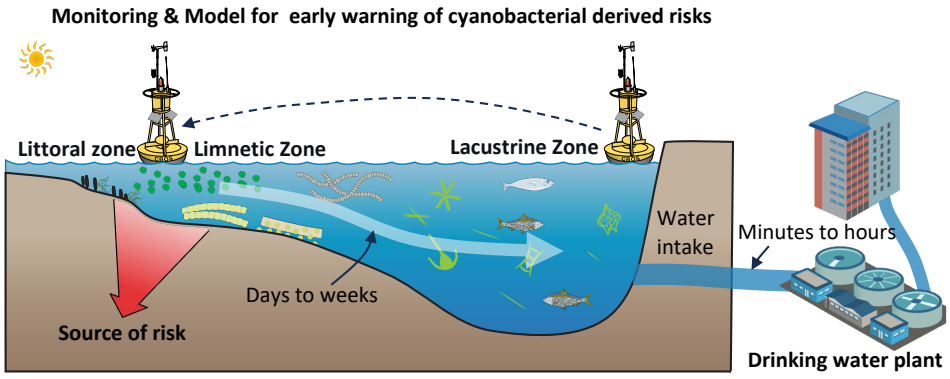

Fig. 6: Conceptual model of littoral-initiated geosmin transport and its implications for monitoring strategy. A sketch illustrating the spatiotemporal progression of geosmin episodes: (1) high metabolic activity of cyanobacteria (e.g., *Planktothrix agardhii*) in the littoral zone, driven by nutrient inputs and favorable light conditions; (2) advection of produced geosmin and biomass into the limnetic zone, resulting in a transport lag; (3) accumulation of geosmin in the lacustrine zone (dam intake), posing an immediate treatment challenge; and (4) the proposed monitoring shift from conventional reactive intake-focused sampling to proactive early detection in littoral zones, providing critical warning time for preventive measures.

utilities can move beyond reactive crisis management—such as emergency high-dose activated carbon application—toward preventive catchment-based strategies. This lead time is further supported by the lagged correlation at YQ01 (R^2 = 0.41 at 5 weeks). This interval allows for optimized treatment costs and proactive resource allocation to intercept risks during the incipient growth phase, aligning with modern water safety frameworks (Recknagel et al., 2017).

This monitoring framework is most applicable to reservoirs where odor production is dominated by littoral hotspots (Izydorczyk et al., 2008). Because the warning lag may vary among systems, it should be calibrated according to reservoir-specific characteristics, including hydrodynamic conditions, shoreline-to-intake distance, water residence time, and the spatial distribution of odor-producing cyanobacteria(Chong et al., 2018; Shin et al., 2022; Song et al., 2023). Systems dominated by deep-water or benthic producers may require modified sentinel-station strategies (Gaget et al., 2020; Izaguirre and Taylor, 2007; Su et al., 2017). In addition, the biomass threshold of 5.0×10^7 cells L^{-1} at YQ05 should be regarded as a preliminary indicator rather than a fixed decision threshold (Almuhtaram et al., 2021; Recknagel et al., 2017). Accordingly, it is better used as a practical reference for sentinel monitoring and early intervention. Exceedance at littoral stations may serve as an early-warning signal to intensify surveillance and, where feasible,

support operational measures such as selective withdrawal or hydrodynamic control to limit the transport of geosmin-rich water toward critical intake depths (Lehman et al., 2009; Song et al., 2023, 2023).

While the current dataset captures robust seasonal and interannual trends, longer-term observations are required to evaluate these dynamics under shifting climate scenarios. Furthermore, while *P. agardhii* is the dominant producer in this system, other reservoirs may be driven by different taxa, such as *Dolichospermum* or *Aphanizomenon* (Choo et al., 2025; Izaguirre and Taylor, 2004; Su et al., 2013).

Future research should focus on: (1) integrating molecular tools to characterize the diversity and expression of geosmin synthesis genes, (2) coupling ecological monitoring with high-resolution hydrodynamic modeling to refine transport time estimates, and (3) conducting cost-benefit analyses to evaluate the economic feasibility of expanded littoral monitoring. By establishing quantifiable early-warning indicators based on the littoral-to-lacustrine transport mechanism, this work provides a technical foundation for improving drinking water security.

5 Conclusions

This study demonstrates that geosmin risk in drinking water reservoirs is governed by a systematic spatiotemporal decoupling, whereby shallow littoral zones function as primary production hotspots, with odor manifestation at the lacustrine intake lagging by several weeks. This quantifiable lag transforms the monitoring paradigm, establishing that proactive surveillance of littoral cyanobacteria provides a critical early-warning window, thereby enabling a shift from reactive treatment toward predictive, source-water management for ensuring drinking water security.

Acknowledgements

This work was financially supported by the National Natural Science Foundation of China (W2412156, 52030002), and Science and Technology Plan Project of Tianjin Water Bureau (JSGJ202031).

References

Ai, Y., Wu, Y., Su, M., Gui, Y., Du, Y., Fang, J., Cao, T., Yang, M., 2025. Cyanobacterial crowding-out effects on metabolite partitioning: Modeling 2-methylisoborneol (MIB) release dynamics and implications. Journal of Hazardous Materials 140118. https://doi.org/10.1016/j.jhazmat.2025.140118

Akbarzadeh, Z., Bocaniov, S.A., Powley, H., Lamb, K.G., Cappellen, P.V., 2025. Mass balance modeling highlights the role of the littoral zone in modulating the cycling of phosphorus in a large, multi-basin lake (lake erie). Journal of Great Lakes Research 51, 102695. https://doi.org/10.1016/j.jglr.2025.102695

Almuhtaram, H., Kibuye, F.A., Ajjampur, S., Glover, C.M., Hofmann, R., Gaget, V., Owen, C., Wert, E.C., Zamyadi, A., 2021. State of knowledge on early warning tools for cyanobacteria detection. Ecological Indicators 133, 108442. https://doi.org/10.1016/j.ecolind.2021.108442

Arora, N.K., Mishra, I., 2022. Sustainable development goal 6: Global water security. Environmental Sustainability 5, 271–275. https://doi.org/10.1007/s42398-022-00246-5

Asato, Y., 2003. Toward an understanding of cell growth and the cell division cycle of unicellular photoautotrophic cyanobacteria. Cellular and Molecular Life Sciences (CMLS) 60, 663–687. https://doi.org/10.1007/s00018-003-2079-y

AWWA, A.W.W.A., 2010. Algae: Source to treatment. American Water Works Association.

Bolyen, E., Rideout, J.R., Dillon, M.R., Bokulich, N.A., Abnet, C.C., Al-Ghalith, G.A., Alexander, H., Alm, E.J., Arumugam, M., Asnicar, F., Bai, Y., Bisanz, J.E., Bittinger, K., Brejnrod, A., Brislawn,

C.J., Brown, C.T., Callahan, B.J., Caraballo-Rodríguez, A.M., Chase, J., Cope, E.K., Da Silva, R., Diener, C., Dorrestein, P.C., Douglas, G.M., Durall, D.M., Duvallet, C., Edwardson, C.F., Ernst, M., Estaki, M., Fouquier, J., Gauglitz, J.M., Gibbons, S.M., Gibson, D.L., Gonzalez, A., Gorlick, K., Guo, J., Hillmann, B., Holmes, S., Holste, H., Huttenhower, C., Huttley, G.A., Janssen, S., Jarmusch, A.K., Jiang, L., Kaehler, B.D., Kang, K.B., Keefe, C.R., Keim, P., Kelley, S.T., Knights, D., Koester, I., Kosciolek, T., Kreps, J., Langille, M.G.I., Lee, J., Ley, R., Liu, Y.-X., Loftfield, E., Lozupone, C., Maher, M., Marotz, C., Martin, B.D., McDonald, D., McIver, L.J., Melnik, A.V., Metcalf, J.L., Morgan, S.C., Morton, J.T., Naimey, A.T., Navas-Molina, J.A., Nothias, L.F., Orchanian, S.B., Pearson, T., Peoples, S.L., Petras, D., Preuss, M.L., Pruesse, E., Rasmussen, L.B., Rivers, A., Robeson, M.S., Rosenthal, P., Segata, N., Shaffer, M., Shiffer, A., Sinha, R., Song, S.J., Spear, J.R., Swafford, A.D., Thompson, L.R., Torres, P.J., Trinh, P., Tripathi, A., Turnbaugh, P.J., Ul-Hasan, S., Hooft, J.J.J. van der, Vargas, F., Vázquez-Baeza, Y., Vogtmann, E., Hippel, M. von, Walters, W., Wan, Y., Wang, M., Warren, J., Weber, K.C., Williamson, C.H.D., Willis, A.D., Xu, Z.Z., Zaneveld, J.R., Zhang, Y., Zhu, Q., Knight, R., Caporaso, J.G., 2019. Reproducible, interactive, scalable and extensible microbiome data science using QIIME 2. Nature Biotechnology 37, 852–857. https://doi.org/10.1038/s41587-019-0209-9

Bracchini, L., Dattilo, A.M., Hull, V., Loiselle, S.A., Tognazzi, A., Rossi, C., 2009. Modelling upwelling irradiance using secchi disk depth in lake ecosystems. Journal of Limnology 68, 83. https://doi.org/10.4081/jlimnol.2009.83

Burlingame, G.A., Doty, R.L., Dietrich, A.M., 2017. Humans as sensors to evaluate drinking water taste and odor: A review. Journal AWWA 109, 13–24. https://doi.org/10.5942/jawwa.2017.109.0118

Cai, F., Yu, G., Zhang, K., Chen, Y., Li, Q., Yang, Y., Xie, J., Wang, Y., Li, R., 2017. Geosmin production and polyphasic characterization of *Oscillatoria limosa* agardh ex gomont isolated from the open canal of a large drinking water system in tianjin city, china. Harmful Algae 69, 28–37. https://doi.org/10.1016/j.hal.2017.09.006

Canizales, S., Sliwszcinka, M., Russo, A., Bentvelzen, S., Temmink, H., Verschoor, A.M., Wijffels,

R.H., Janssen, M., 2021. Cyanobacterial growth and cyanophycin production with urea and ammonium as nitrogen source. Journal of Applied Phycology 33, 3565–3577. https://doi.org/10.1007/s10811-021-02575-0

Cao, T., Su, M., Ai, Y., Yang, Z., Zhao, J., Yang, M., 2025. Green light suppresses cell growth but enhances photosynthetic rate and MIB biosynthesis in PE-containing pseudanabaena. Water Research 123336. https://doi.org/10.1016/j.watres.2025.123336

Carmichael, W.W., Azevedo, S.M., An, J.S., Molica, R.J., Jochimsen, E.M., Lau, S., Rinehart, K.L., Shaw, G.R., Eaglesham, G.K., 2001. Human fatalities from cyanobacteria: Chemical and biological evidence for cyanotoxins. Environmental Health Perspectives 109, 663–668. https://doi.org/10.1289/ehp.01109663

Cefalì, M.E., Cebrian, E., Chappuis, E., Pinedo, S., Terradas, M., Mariani, S., Ballesteros, E., 2016. Life on the boundary: Environmental factors as drivers of habitat distribution in the littoral zone. Estuarine, Coastal and Shelf Science 172, 81–92. https://doi.org/10.1016/j.ecss.2016.01.043

Cerón-Vivas, A., Villamizar León, M.P., Cajigas, Á.A., 2022. Geosmin and 2-methylisoborneol removal in drinking water treatment. Water Practice and Technology 18, 159–167. https://doi.org/10.2166/wpt.2022.167

Chislock, M.F., Olsen, B.K., Choi, J., Abebe, A., Bleier, T.L., Wilson, A.E., 2021. Contrasting patterns of 2-methylisoborneol (MIB) vs. Geosmin across depth in a drinking water reservoir are mediated by cyanobacteria and actinobacteria. Environmental Science and Pollution Research. https://doi.org/10.1007/s11356-021-12973-z

Chong, S., Lee, H., An, K.-G., 2018. Predicting taste and odor compounds in a shallow reservoir using a three–dimensional hydrodynamic ecological model. Water 10, 1396. https://doi.org/10.3390/w10101396

Choo, F., Cook, D., Hobson, P., 2025. Investigating the physicochemical parameters that drive geosmin production in benthic cyanobacterial systems. Water Research 287, 124388. https://doi.org/10.1016/j.watres.2025.124388

Churro, C., Semedo-Aguiar, A.P., Silva, A.D., Pereira-Leal, J.B., Leite, R.B., 2020. A novel cyanobacterial geosmin producer, revising GeoA distribution and dispersion patterns in bacteria. Scientific Reports 10. https://doi.org/10.1038/s41598-020-64774-y

Clercin, N.A., Druschel, G.K., Gray, M., 2021. Occurrences of 2-methylisoborneol and geosmin –degrading bacteria in a eutrophic reservoir and the role of cell-bound versus dissolved fractions. Journal of Environmental Management 297, 113304. https://doi.org/10.1016/j.jenvman.2021.113304

Cook, D., Newcombe, G., Sztajnbok, P., 2001. The application of powdered activated carbon for MIB and geosmin removal: Predicting PAC doses in four raw waters. Water Research 35, 1325–1333. https://doi.org/10.1016/S0043-1354(00)00363-8

Devi, A., Chiu, Y.-T., Hsueh, H.-T., Lin, T.-F., 2021. Quantitative PCR based detection system for cyanobacterial geosmin/2-methylisoborneol (2-MIB) events in drinking water sources: Current status and challenges. Water Research 188, 116478. https://doi.org/10.1016/j.watres.2020.116478

Dordoni, M., Zappalà, P., Barth, J.A.C., 2023. A preliminary global hydrochemical comparison of lakes and reservoirs. Frontiers in Water 5. https://doi.org/10.3389/frwa.2023.1084050

Dubourg, P., North, R.L., Hunter, K., Vandergucht, D.M., Abirhire, O., Silsbe, G.M., Guildford, S.J., Hudson, J.J., 2015. Light and nutrient co-limitation of phytoplankton communities in a large reservoir: Lake diefenbaker, saskatchewan, canada. Journal of Great Lakes Research 41, 129–143. https://doi.org/10.1016/j.jglr.2015.10.001

Edgar, R.C., 2013. UPARSE: Highly accurate OTU sequences from microbial amplicon reads. Nature Methods 10, 996–998. https://doi.org/10.1038/nmeth.2604

Feng, L., Dai, Y., Hou, X., Xu, Y., Liu, J., Zheng, C., 2021. Concerns about phytoplankton bloom trends in global lakes. Nature 590, E35–E47. https://doi.org/10.1038/s41586-021-03254-3

Flores, E., Herrero, A., 2005. Nitrogen assimilation and nitrogen control in cyanobacteria. Biochemical Society Transactions 33, 164–167. https://doi.org/10.1042/bst0330164

Gaget, V., Hobson, P., Keulen, A., Newton, K., Monis, P., Humpage, A.R., Weyrich, L.S., Brookes,

J.D., 2020. Toolbox for the sampling and monitoring of benthic cyanobacteria. Water Research 169, 115222. https://doi.org/10.1016/j.watres.2019.115222

Gerber, N.N., 1979. Volatile Substances from Actinomycetes: Their Role in the Odor Pollution of Water. CRC Critical Reviews in Microbiology 7, 191–214. https://doi.org/10.3109/10408417909082014

Gerber, N.N., Lechevalier, H.A., 1965. Geosmin, an earthy-smelling substance isolated from actinomycetes. Applied Microbiology 13, 935–938.

Giglio, S., Chou, W.K.W., Ikeda, H., Cane, D.E., Monis, P.T., 2011. Biosynthesis of 2-methylisoborneol in cyanobacteria. Environmental Science & Technology 45, 992–998. https://doi.org/10.1021/es102992p

Giglio, S., Jiang, J., Saint, C.P.S., Cane, D.E., Monis, P.T., 2008. Isolation and characterization of the gene associated with geosmin production in cyanobacteria. Environmental Science & Technology 42, 8027–8032. https://doi.org/10.1021/es801465w

Guo, H., Li, R., Xue, S., Zhangsun, X., Huang, D., Li, Y., Li, N., Su, Y., Zhang, H., Huang, T., 2024. Considerable declines in odor in a drinking water reservoir: Variations of odorous community, precursor enzymes abundance, distribution, and environmental dominant factors. Water Research 122767. https://doi.org/10.1016/j.watres.2024.122767

Hammond, D., Murri, A., Mastitsky, S., Yang, Z., Foster, R., Schweitzer, L., 2021. Geosmin reduction by algaecide application to drinking water: Field scale efficacy and mechanistic insights. Heliyon 7, e07706. https://doi.org/10.1016/j.heliyon.2021.e07706

Hawkins, P.R., Holliday, J., Kathuria, A., Bowling, L., 2005. Change in cyanobacterial biovolume due to preservation by lugol's iodine. Harmful Algae 4, 1033–1043. https://doi.org/10.1016/j.hal.2005.03.001

Hayashi, S., Ohtani, S., Godo, T., Nojiri, Y., Saki, Y., Esumi, T., Kamiya, H., 2019. Identification of geosmin biosynthetic gene in geosmin-producing colonial cyanobacteria coelosphaerium sp. And isolation of geosmin non-producing coelosphaerium sp. From brackish lake shinji in japan. Harmful Algae 84, 19–26. https://doi.org/10.1016/j.hal.2019.01.010

Heisler, J., Glibert, P.M., Burkholder, J.M., Anderson, D.M., Cochlan, W., Dennison, W.C., Dortch, Q., Gobler, C.J., Heil, C.A., Humphries, E., Lewitus, A., Magnien, R., Marshall, H.G., Sellner, K., Stockwell, D.A., Stoecker, D.K., Suddleson, M., 2008. Eutrophication and harmful algal blooms: A scientific consensus. Harmful Algae 8, 3–13. https://doi.org/10.1016/j.hal.2008.08.006

Hoefel, D., Ho, L., Monis, P.T., Newcombe, G., Saint, C.P., 2009. Biodegradation of geosmin by a novel gram-negative bacterium; isolation, phylogenetic characterisation and degradation rate determination. Water Research 43, 2927–2935. https://doi.org/10.1016/j.watres.2009.04.005

Holgerson, M.A., Richardson, D.C., Roith, J., Bortolotti, L.E., Finlay, K., Hornbach, D.J., Gurung, K., Ness, A., Andersen, M.R., Bansal, S., Finlay, J.C., Cianci-Gaskill, J.A., Hahn, S., Janke, B.D., McDonald, C., Mesman, J.P., North, R.L., Roberts, C.O., Sweetman, J.N., Webb, J.R., 2022. Classifying mixing regimes in ponds and shallow lakes. Water Resources Research 58. https://doi.org/10.1029/2022wr032522

Hooper, A.S., Kille, P., Watson, S.E., Christofides, S.R., Perkins, R.G., 2023. The importance of nutrient ratios in determining elevations in geosmin synthase (geoA) and 2-MIB cyclase (mic) resulting in taste and odour events. Water Research 119693. https://doi.org/10.1016/j.watres.2023.119693

Hu, H.J., Wei, Y.X., 2006. The freshwater algae of china-systematics, taxonomy and ecology. Science Press, Beijing, China.

Huisman, J., Codd, G.A., Paerl, H.W., Ibelings, B.W., Verspagen, J.M.H., Visser, P.M., 2018. Cyanobacterial blooms. Nature Reviews Microbiology 16, 471–483. https://doi.org/10.1038/s41579-018-0040-1

Izaguirre, G., 1992. A copper-tolerant phormidium species from lake mathews, california, that produces 2-methylisoborneol and geosmin. Water Science and Technology 25, 217–223. https://doi.org/10.2166/wst.1992.0055

Izaguirre, G., Taylor, W.D., 2007. Geosmin and MIB events in a new reservoir in southern califor-

583 nia. Water Science and Technology 55, 9–14. https://doi.org/10.2166/wst.2007.156
584 Izaguirre, G., Taylor, W.D., 2004. A guide to geosmin- and MIB-producing cyanobacteria in the
585 united states. Water Science and Technology 49, 19–24. https://doi.org/10.2166/wst.2004.
586 0524
587 Izydorczyk, K., Skowron, A., Wojtal, A., Jurczak, T., 2008. The stream inlet to a shallow bay of a
588 drinking water reservoir, a “hot-spot” forMicrocystisBlooms initiation. International Review
589 of Hydrobiology 93, 257–268. https://doi.org/10.1002/iroh.200710959
590 Jensen, S., Anders, C., Goatcher, L., Perley, T., Kenefick, S., Hrudey, S., 1994. Actinomycetes as a
591 factor in odour problems affecting drinking water from the north saskatchewan river. Water
592 Research 28, 1393–1401. https://doi.org/0043-1354(94)90306-9
593 Jia, Z., Su, M., Liu, T., Guo, Q., Wang, Q., Burch, M., Yu, J., Yang, M., 2019. Light as a possible
594 regulator of MIB-producing planktothrix in source water reservoir, mechanism and in-situ
595 verification. Harmful Algae 88, 101658. https://doi.org/10.1016/j.hal.2019.101658
596 John, N., Koehler, A.V., Ansell, B.R.E., Baker, L., Crosbie, N.D., Jex, A.R., 2018. An improved
597 method for PCR-based detection and routine monitoring of geosmin-producing cyanobac-
598 terial blooms. Water Research 136, 34–40. https://doi.org/10.1016/j.watres.2018.02.041
599 Jüttner, F., Watson, S.B., 2007. Biochemical and ecological control of geosmin and 2-
600 methylisoborneol in source waters. Applied and Environmental Microbiology 73, 4395–4406.
601 https://doi.org/10.1128/aem.02250-06
602 Kim, T.-K., Moon, B.-R., Kim, T., Kim, M.-K., Zoh, K.-D., 2016. Degradation mechanisms of
603 geosmin and 2-MIB during UV photolysis and UV/chlorine reactions. Chemosphere 162,
604 157–164. https://doi.org/10.1016/j.chemosphere.2016.07.079
605 Komárek, J., Johansen, J.R., 2015. Chapter 4 - filamentous cyanobacteria, in: Freshwater Algae
606 of North America (Second Edition). Academic Press, Boston, pp. 135–235. https://doi.org/
607 10.1016/b978-0-12-385876-4.00004-9
608 Kosten, S., Huszar, V.L.M., Bécares, E., Costa, L.S., Donk, E. van, Hansson, L., Jeppesen, E., Kruk,
609 C., Lacerot, G., Mazzeo, N., De Meester, L., Moss, B., Lürling, M., Nõges, T., Romo, S., Scheffer,

M., 2011. Warmer climates boost cyanobacterial dominance in shallow lakes. Global Change Biology 18, 118–126. https://doi.org/10.1111/j.1365-2486.2011.02488.x

Kutovaya, O.A., Watson, S.B., 2014. Development and application of a molecular assay to detect and monitor geosmin-producing cyanobacteria and actinomycetes in the great lakes. Journal of Great Lakes Research 40, 404–414. https://doi.org/10.1016/j.jglr.2014.03.016

Lehman, E.M., McDonald, K.E., Lehman, J.T., 2009. Whole lake selective withdrawal experiment to control harmful cyanobacteria in an urban impoundment. Water Research 43, 1187–1198. https://doi.org/10.1016/j.watres.2008.12.007

Lin, T.-F., Watson, S., Suffet, I.H.M., 2018. Taste and odour in source and drinking water: Causes, controls, and consequences. IWA Publishing.

Lu, J., Su, M., Su, Y., Fang, J., Burch, M., Cao, T., Wu, B., Yu, J., Yang, M., 2023. MIB-derived odor management based upon hydraulic regulation in small drinking water reservoirs: Principle and application. Water Research 244, 120485. https://doi.org/10.1016/j.watres.2023.120485

Mehnert, G., Leunert, F., Cires, S., Johnk, K.D., Rucker, J., Nixdorf, B., Wiedner, C., 2010. Competitiveness of invasive and native cyanobacteria from temperate freshwaters under various light and temperature conditions. Journal of Plankton Research 32, 1009–1021. https://doi.org/10.1093/plankt/fbq033

Merel, S., Walker, D., Chicana, R., Snyder, S., Baurès, E., Thomas, O., 2013. State of knowledge and concerns on cyanobacterial blooms and cyanotoxins. Environment International 59, 303–327. https://doi.org/10.1016/j.envint.2013.06.013

Mohanty, S., Pandey, P.C., Srivastava, P.K., Srivastava, S.K., 2024. Challenges and future implications in monitoring and assessment of aquatic ecosystems, in: Aquatic Ecosystems Monitoring. CRC Press, pp. 297–318.

Mustapha, S., Tijani, J.O., Ndamitso, M., Abdulkareem, A.S., Shuaib, D.T., Mohammed, A.K., 2021. A critical review on geosmin and 2-methylisoborneol in water: Sources, effects, detection, and removal techniques. Environmental Monitoring and Assessment 193. https://doi.org/

637 10.1007/s10661-021-08980-9
638 O'neil, J.m., Davis, T.w., Burford, M.a., Gobler, C.j., 2012. The rise of harmful cyanobacteria
639 blooms: The potential roles of eutrophication and climate change. Harmful Algae 14, 313–
640 334. https://doi.org/10.1016/j.hal.2011.10.027
641 Paerl, H.W., Fulton, R.S., Moisander, P.H., Dyble, J., 2001. Harmful freshwater algal blooms, with
642 an emphasis on cyanobacteria. The Scientific World Journal 1, 76–113. https://doi.org/10.
643 1100/tsw.2001.16
644 Paerl, H.W., Paul, V.J., 2012. Climate change: Links to global expansion of harmful cyanobacteria.
645 Water Research 46, 1349–1363. https://doi.org/10.1016/j.watres.2011.08.002
646 Paerl, H.W., Xu, H., Mccarthy, M.J., Zhu, G., Qin, B., Li, Y., Gardner, W.S., 2011. Controlling harmful
647 cyanobacterial blooms in a hyper-eutrophic lake (lake taihu, China): The need for a dual
648 nutrient (n & p) management strategy. Water Research 45, 1973–1983. https://doi.org/10.
649 1016/j.watres.2010.09.018
650 Pham, T.-L., Bui, M.H., Driscoll, M., Shimizu, K., Motoo, U., 2020. First report of geosmin and 2-
651 methylisoborneol (2-MIB) in *Dolichospermum* and *Oscillatoria* from vietnam. Limnology 22,
652 43–56. https://doi.org/10.1007/s10201-020-00630-2
653 Plaas, H.E., Paerl, H.W., 2020. Toxic cyanobacteria: A growing threat to water and air quality.
654 Environmental Science & Technology 55, 44–64. https://doi.org/10.1021/acs.est.0c06653
655 Qin, B., Yang, L., Chen, F., Zhu, G., Zhang, L., Chen, Y., 2006. Mechanism and control of lake
656 eutrophication. Chinese Science Bulletin 51, 2401–2412. https://doi.org/10.1007/s11434-
657 006-2096-y
658 Qiu, P., Chen, Y., Li, C., Huo, D., Bi, Y., Wang, J., Li, Y., Li, R., Yu, G., 2021. Using molecular detec-
659 tion for the diversity and occurrence of cyanobacteria and 2-methylisoborneol-producing
660 cyanobacteria in an eutrophicated reservoir in Northern China. Environmental Pollution
661 288, 117772. https://doi.org/10.1016/j.envpol.2021.117772
662 Qiu, P., Zhang, Y., Mi, W., Song, G., Bi, Y., 2023. Producers and drivers of odor compounds in a
663 large drinking-water source. Frontiers in Ecology and Evolution 11. https://doi.org/10.3389/

fevo.2023.1216567

Quast, C., Pruesse, E., Yilmaz, P., Gerken, J., Schweer, T., Yarza, P., Peplies, J., Glöckner, F.O., 2012. The SILVA ribosomal RNA gene database project: Improved data processing and web-based tools. Nucleic Acids Research 41, D590–D596. https://doi.org/10.1093/nar/gks1219

Ravi, R.K., Walton, K., Khosroheidari, M., 2018. MiSeq: A next generation sequencing platform for genomic analysis, in: Disease Gene Identification. Springer New York, pp. 223–232. https://doi.org/10.1007/978-1-4939-7471-9_12

Recknagel, F., Orr, P.T., Bartkow, M., Swanepoel, A., Cao, H., 2017. Early warning of limit-exceeding concentrations of cyanobacteria and cyanotoxins in drinking water reservoirs by inferential modelling. Harmful Algae 69, 18–27. https://doi.org/10.1016/j.hal.2017.09.003

Reinl, K.L., Harris, T.D., Elfferich, I., Coker, A., Zhan, Q., Domis, L.N.D.S., Morales-Williams, A.M., Bhattacharya, R., Grossart, H.-P., North, R.L., Sweetman, J.N., 2022. The role of organic nutrients in structuring freshwater phytoplankton communities in a rapidly changing world. Water Research 219, 118573. https://doi.org/10.1016/j.watres.2022.118573

Rousso, B.Z., Bertone, E., Stewart, R., Hamilton, D.P., 2020. A systematic literature review of forecasting and predictive models for cyanobacteria blooms in freshwater lakes. Water Research 182, 115959. https://doi.org/10.1016/j.watres.2020.115959

Saadoun, I.M.K., Schrader, K.K., Blevins, W.T., 2001. Environmental and nutritional factors affecting geosmin synthesis by Anabaena sp. Water Research 35, 1209–1218. https://doi.org/10.1016/S0043-1354(00)00381-X

Scott, J.T., Marcarelli, A.M., 2012. Cyanobacteria in freshwater benthic environments, in: Ecology of Cyanobacteria Ii. Springer Netherlands, pp. 271–289. https://doi.org/10.1007/978-94-007-3855-3_9

Shin, J.-K., Park, Y., Kim, N.-Y., Hwang, S.-J., 2022. Downstream transport of geosmin based on harmful cyanobacterial outbreak upstream in a reservoir cascade. International Journal of Environmental Research and Public Health 19, 9294. https://doi.org/10.3390/ijerph19159294

691 Singh, S., Kate, B.N., Banerjee, U.C., 2005. Bioactive compounds from cyanobacteria
692 and microalgae: An overview. Critical Reviews in Biotechnology 25, 73–95. https:
693 //doi.org/10.1080/07388550500248498
694 Song, Y., Chen, M., Li, J., Zhang, L., Deng, Y., Chen, J., 2023. Can selective withdrawal control
695 algal blooms in reservoirs? The underlying hydrodynamic mechanism. Journal of Cleaner
696 Production 394, 136358. https://doi.org/10.1016/j.jclepro.2023.136358
697 Soyluoglu, M., Kim, D., Zaker, Y., Karanfil, T., 2022. Removal mechanisms of geosmin and MIB by
698 oxygen nanobubbles during water treatment. Chemical Engineering Journal 443, 136535.
699 https://doi.org/10.1016/j.cej.2022.136535
700 Srinivasan, R., Sorial, G.A., 2011. Treatment of taste and odor causing compounds 2-methyl
701 isoborneol and geosmin in drinking water: A critical review. Journal of Environmental Sci-
702 ences 23, 1–13. https://doi.org/10.1016/s1001-0742(10)60367-1
703 Su, M., Andersen, T., Burch, M., Jia, Z., An, W., Yu, J., Yang, M., 2019. Succession and interaction
704 of surface and subsurface cyanobacterial blooms in oligotrophic/mesotrophic reservoirs: A
705 case study in Miyun Reservoir. Science of the Total Environment 649, 1553–1562. https://
706 doi.org/J.scitotenv.2018.08.307
707 Su, M., Gaget, V., Giglio, S., Burch, M., An, W., Yang, M., 2013. Establishment of quantitative
708 PCR methods for the quantification of geosmin-producing potential and *Anabaena* sp. In
709 freshwater systems. Water Research 47, 3444–3454. https://doi.org/10.1016/j.watres.2013.
710 03.043
711 Su, M., Jia, D., Yu, J., Vogt, R.D., Wang, J., An, W., Yang, M., 2017. Reducing production of taste and
712 odor by deep-living cyanobacteria in drinking water reservoirs by regulation of water level.
713 Science of The Total Environment 574, 1477–1483. https://doi.org/10.1016/j.scitotenv.2016.
714 08.134
715 Su, M., Yu, J., Zhang, J., Chen, H., An, W., Vogt, R.D., Andersen, T., Jia, D., Wang, J., Yang, M.,
716 2015. MIB-producing cyanobacteria (*Planktothrix* sp.) in a drinking water reservoir: Distri-
717 bution and odor producing potential. Water Research 68, 444–453. https://doi.org/10.1016/

j.watres.2014.09.038

Sun, D., Yu, J., Yang, M., An, W., Zhao, Y., Lu, N., Yuan, S., Zhang, D., 2014. Occurrence of odor problems in drinking water of major cities across China. Frontiers of Environmental Science & Engineering 8, 411–416. https://doi.org/10.1007/s11783-013-0577-1

Suurnäkki, S., Gomez-saez, G.V., Rantala-ylinen, A., Jokela, J., Fewer, D.P., Sivonen, K., 2015. Identification of geosmin and 2-methylisoborneol in cyanobacteria and molecular detection methods for the producers of these compounds. Water Research 68, 56–66. https://doi.org/10.1016/j.watres.2014.09.037

Thornton, K.W., 1984. REGIONAL COMPARISONS OF LAKES AND RESERVOIRS: GEOLOGY, CLIMATOLOGY, AND MORPHOLOGY. Lake and Reservoir Management 1, 261–265. https://doi.org/10.1080/07438148409354521

Watson, S.B., 2003. Cyanobacterial and eukaryotic algal odour compounds: Signals or by-products? A review of their biological activity. Phycologia 42, 332–350. https://doi.org/10.2216/i0031-8884-42-4-332.1

Woolway, R.I., Kraemer, B.M., Lenters, J.D., Merchant, C.J., O'Reilly, C.M., Sharma, S., 2020. Global lake responses to climate change. Nature Reviews Earth & Environment 1, 388–403. https://doi.org/10.1038/s43017-020-0067-5

Wu, T., Zhu, G., Wang, Z., Zhu, M., Xu, H., 2022. Seasonal dynamics of odor compounds concentration driven by phytoplankton succession in a subtropical drinking water reservoir, southeast China. Journal of Hazardous Materials 425, 128056. https://doi.org/10.1016/j.jhazmat.2021.128056

Xu, H., Paerl, H.W., Qin, B., Zhu, G., Gaoa, G., 2009. Nitrogen and phosphorus inputs control phytoplankton growth in eutrophic Lake Taihu, China. Limnology and Oceanography 55, 420–432. https://doi.org/10.4319/lo.2010.55.1.0420

Xu, Y., Xie, R., Wang, Y., Sha, J., 2014. Spatio-temporal variations of water quality in yuqiao reservoir basin, north china. Frontiers of Environmental Science & Engineering 9, 649–664. https://doi.org/10.1007/s11783-014-0702-9

Yang, M., Yu, J., Li, Z., Guo, Z., Burch, M., Lin, T., 2008. Taihu Lake not to blame for Wuxi's Woes. Science 319, 158. https://doi.org/10.1126/science.319.5860.158a

Yang, X., Dong, W., Liu, L., Bi, Y., Xu, W., Wang, X., 2023. Uncovering the differential growth of microcystis aeruginosa cultivated under nitrate and ammonium from a photophysiological perspective. ACS ES&T Water 3, 1161–1171. https://doi.org/10.1021/acsestwater.2c00624

Yuan, J., Hofmann, R., 2022. Adsorption and biodegradation of 2-methylisoborneol and geosmin in drinking water granular activated carbon filters: A review and meta-analysis. Journal of Hazardous Materials 440, 129838. https://doi.org/10.1016/j.jhazmat.2022.129838

Zamyadi, A., Henderson, R., Stuetz, R., Hofmann, R., Ho, L., Newcombe, G., 2015. Fate of geosmin and 2-methylisoborneol in full-scale water treatment plants. Water Research 83, 171–183. https://doi.org/10.1016/j.watres.2015.06.038

Zhai, H., He, X., Zhang, Y., Du, T., Adeleye, A.S., Li, Y., 2017. Disinfection byproduct formation in drinking water sources: A case study of yuqiao reservoir. Chemosphere 181, 224–231. https://doi.org/10.1016/j.chemosphere.2017.04.028

Zhang, Y., Whalen, J.K., Cai, C., Shan, K., Zhou, H., 2023. Harmful cyanobacteria-diatom/dinoflagellate blooms and their cyanotoxins in freshwaters: A nonnegligible chronic health and ecological hazard. Water Research 233, 119807. https://doi.org/10.1016/j.watres.2023.119807

Zhou, S., Qiu, D., Xiao, L., 2024. Spatial distribution and influencing factors of organic odorants 2-methylisoborneol and geosmin in reservoirs of guangdong province. Guangdong Chemical Industry (In Chinese) 51, 117–119, 122.

Zohary, T., Gasith, A., 2014. The littoral zone, in: Lake Kinneret. Springer Netherlands, pp. 517–532. https://doi.org/10.1007/978-94-017-8944-8_29